Transactions on Biomedicine and Health vol 1, © 1993 WIT Press, www.witpress.com, ISSN 1743-3525

A transient analysis of human coronary artery blood flow

P.R. Johnston & D. Kilpatrick
Department of Medicine, University of Tasmania, 43 Collins St., Hobart, Tasmania 7000, Australia

ABSTRACT

Despite its prevalence, little is known about the initiating factors for coronary artery disease. Physical factors associated with blood flow have been implicated with some believing that regions of low wall shear stress predispose to atheroma and subsequent narrowing, but others believe that narrowing is initiated by high shear stress.

This paper presents a modelling study of blood flowing through the first main junction in the left side of the human coronary artery tree, involving the left main stem, the left anterior descending (LAD) and the left circumflex arteries (LCA). The eventual aim is to find a correlation between regions of calculated high and low wall shear stress and the position of arterial narrowing.

The paper presents results of transient and steady state simulations performed at various Reynolds numbers. Results are discussed in terms of the magnitude and position of wall shear stress and flow separation at various positions in the arterial junction.

INTRODUCTION

Coronary artery disease is one of the major causes of death in western society and at present its initiating factors are still unknown. Some authors believe it is due to high wall shear stress (Fry, [1]), but others believe it is due to low wall shear stress (Caro et al., [2]). This paper presents a modelling study of the fluid mechanics of blood flow in a bifurcation of a coronary artery with a view to predicting regions of high and low wall shear stress. The ultimate aim is to correlate these regions with areas of arterial narrowing observed from angiograms (X–ray pictures of the heart containing contrast medium in the blood vessel). This will provide an answer to the question of whether

arterial geometry is associated with subsequent arterial stenosis.

The next sections contain some background to experimental and modelling studies of blood flow in arteries and the solution technique used to obtain the flow patterns and related quantities. The final section presents the results of the simulations performed.

BACKGROUND

Fatty streaks occurring in the arterial wall have been shown (Stary, [3]) to lead to the true atheromatous plaques that form coronary artery disease. These streaks are known to be preferentially distributed at certain sites on the arterial walls. In particular these are the outer walls of arterial junctions and the inside of walls of curves. The non–uniform distribution of the fatty streaks suggests a position dependent wall permeability, enabling transport of cholesterol bearing lipoproteins in and out of the wall.

It has been shown that (Fry, [1]) if the arterial wall is subjected to (unphysiologically) high wall shear stress for a short period of time, the lining of the artery is irreversibly damaged and its permeability increases. This leads to the conclusion that high shear damage might be an initiating factor in coronary artery disease. Alternatively, it has also been shown (Caro et al., [2]) that fatty streaks develop in regions where low wall shear stress would be expected, given steady flow. This is consistent with the hypothesis that fatty streaks and early atheromatous plaques occur in regions of low wall shear stress.

A resolution to the shear stress question has been attempted experimentally (Asakura and Karino, [4]). Flow patterns in arteries from postmortem hearts, rendered transparent with ethanol and oil of wintergreen, were recorded by tracking polystyrene microspheres (in a suspension of oil of wintergreen and 5% ethanol) with 16–mm cine camera. Five different coronary artery trees were obtained, all from people whose primary cause of death was not cardiovascular disease, where the geometric integrity of the coronary trees was maintained by fixing them to a wire frame. The conclusion reached was that regions of slow or disturbed flow were associated with sites of narrowing.

Modelling blood flow in artery bifurcations using techniques of computational fluid dynamics is not new, but most attention has been directed to the flow through the carotid artery bifurcation (in the neck) (Rindt et al., [5], Perktold and Resch, [6], Perktold et al., [7]). These studies predict regions of flow separation and regions of high and low shear stress. They conclude that observed regions of low shear stress correlate with surgical findings on the location of narrowings. One recent study has looked at blood flow in the a single coronary artery containing only a slight

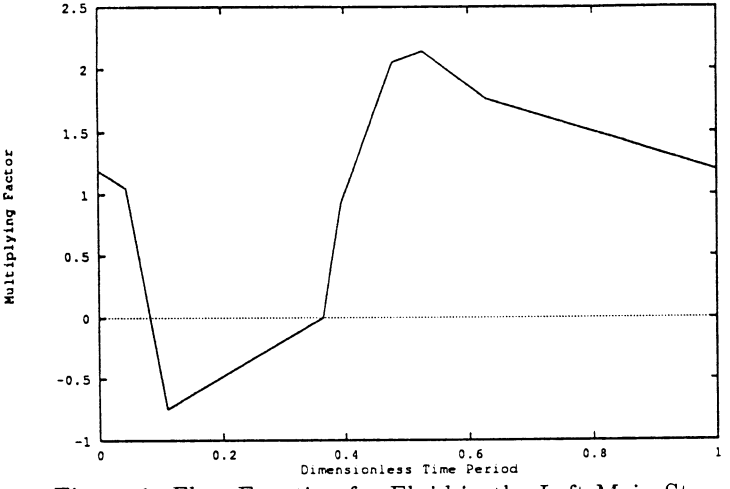


Figure 1: Flow Function for Fluid in the Left Main Stem

curve and taper (Perktold et al., [8]). From this study the importance of the secondary flows in the artery was emphasised, along with their relation to the wall shear stress and subsequent narrowing. The junction considered here is that of the left main stem, left circumflex and left anterior descending arteries, which was chosen because of the high degree of arterial narrowing observed in the vicinity.

SOLUTION METHOD

Blood flow through the coronary arteries is assumed to be governed by the Navier–Stokes and continuity equations. The fluid is considered incompressible and the modelling is performed both transiently and at steady state. In rectangular coordinates the dimensionless governing equations are given by:

$$\frac{\partial \mathbf{v}}{\partial \mathbf{t}} + \mathbf{v} \cdot \nabla \mathbf{v} = \frac{1}{Re} \nabla^2 \mathbf{v} - \nabla p \tag{1}$$

and

$$\nabla \cdot \mathbf{v} = 0 \tag{2}$$

where $\mathbf{v}$ is the velocity vector, p the pressure and Re the Reynolds number. The equations have been rendered dimensionless with respect to D, the arterial diameter at the entrance and U, the average inlet velocity, also at the entrance. Hence the Reynolds number is given by $Re = \frac{\rho DU}{\mu}$, where ρ is the density of blood and μ the blood viscosity, assumed constant.

The boundary conditions are such that there is no flow along the solid walls of the artery (no–slip condition). At the inlet, the fluid is assumed to have a fully developed Hagen–Poiseuille paraboloidal flow field. For the steady state problem this profile is assumed constant, whereas for the transient problem the magnitude of the centerline velocity is scaled according

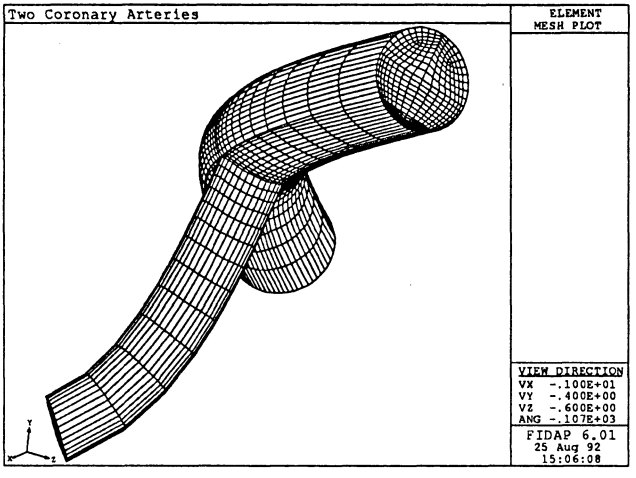


Figure 2: Finite Element Mesh for the Arterial Junction

to the flow function in Fig. 1 (Perktold et al., [8]), whilst maintaining the paraboloidal field. There are two outflow boundaries for this problem. At the first, the continuation of the main artery, the flow is again assumed to have a paraboloidal velocity field, scaled, at any time, to be half of the inlet velocity, thus reflecting the 50–50 flow divide between the two arteries. At the second outflow boundary, stress free boundary conditions are applied and the pressure is set to zero for reference.

The governing equations are solved using the commercially available computational fluid dynamics package, FIDAP, based on the Galerkin finite element method (Engelman, [9], Engelman, [10]). The equations are discretised on a non–uniform grid of approximately 13000 linear brick elements (Fig. 2). Most of the elements are concentrated around the bifurcation point, increasing in size away from the junction. Elements are also concentrated near the walls of the arteries. A system of algebraic equations is obtained from the mesh points and element connectivity by integrating the shape functions from the Galerkin weighted residual representation of the governing equations. The pressure degree of freedom has been eliminated using a penalty function formulation (parameter, $\epsilon = 1 \times 10^{-6}$) and is recovered after the velocities have been calculated, thus reducing the size of the system of equations. A segregated solver, based on the conjugate gradient method, then solves the system of equations iteratively. The transient problem is solved using an implicit backward Euler time integration with variable time steps. At each time step a nonlinear system of equations is solved via the method described above.

There are two important assumptions in the model described above. The

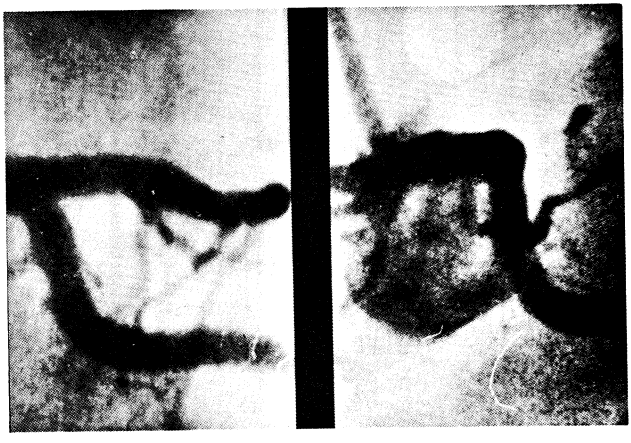


Figure 3: Two Perpendicular Views of the Arterial Junction Considered

first is that blood is a Newtonian fluid. Blood can be considered to be a Newtonian fluid only at high shear rates, because, at low shear, the shear rate – shear stress relationship curves towards the origin. The use of the Newtonian model is justified by the presence of high shear stresses in the modelling situation. Clearly, incorporating a non–Newtonian model would be an improvement. Secondly, the assumption of rigid arterial walls is justified by observing that most of the flow occurs during diastole when the heart is relaxed and the arteries are not subjected to external pressures. Also, the coronary arteries are the least elastic arteries in the body (Fischer and Llaurado, [11]) and so changes in dimension are small during the cardiac cycle.

The coronary artery junction was constructed from two mutually perpendicular angiograms, Fig. 3. Each angiogram of the arterial tree was digitised and the pairs of points matched in three dimensional space, thus providing the centerline of the arterial junction. The full three dimensional structure was reconstructed using PATRAN under the assumption that the arteries have circular cross–sections. A finite element mesh of approximately 12000 nodes was then created, also using PATRAN (Fig. 2).

The most important quantity to be derived from the analysis is the wall shear stress. For incompressible fluids and no–slip conditions at the rigid wall, the dimensionless wall shear stress is

$$\tau_w = \frac{1}{Re} \left. \frac{\partial \mathbf{v}_t}{\partial n} \right|_{wall} \tag{3}$$

where $\partial \mathbf{v}_t / \partial n$ is the partial derivative of the tangential velocity in the nor-

mal direction at the wall.

SIMULATIONS

The simulations performed represent various physical situations occurring in the human body. In all, five simulations were performed, four at steady state and one transiently. The Reynolds number was the only parameter to be varied in this study, taking the values of 15, 75, 150 and 300 in steady state simulations with 50% of the volumetric flow leaving the LCA. Changing the Reynolds number is equivalent to changing the work rate of the heart. As the heart beats faster, due to exercise or stress, the blood flows with increased velocity, thus increasing the Reynolds number. The transient simulation was performed at an average Reynolds number of 75, rising to a peak value of 170, during diastole, again with 50% of the blood leaving via the LCA.

RESULTS

From the steady state simulations it was found that there is a region of high wall shear stress on the downstream side of the LCA as well as another region slightly upstream from the junction in the left main stem. This is typical of flow through any straight T–section junction, except that the symmetry is missing. Regions of low shear stress are on the upstream side of the LCA and a very small region just above the junction, on the main arterial wall.

Perhaps of greater interest are not the regions of extreme high shear stress but those of moderately high values. A region of moderately high wall shear stress occurs further downstream of the junction near the top of LCA. Opposite to this is a region of low wall shear stress. These two regions occur due to the curvature in the LAD, downstream from the junction. A similar pair of regions of high and low wall shear stress occur towards the exit of the flow domain in the LCA, again due to the curvature of the artery.

Values of the maximum wall shear stress at the various Reynolds numbers consider are as follows (given in order of increasing Reynolds number): 18.6, 31.7, 41.0 and 50.4. As would probably be expected, the maximum shear increases with increasing Reynolds number.

Another aspect of the fluid motion to consider is flow separation and recirculation. Flow separation occurs (for steady state simulations) on the upstream side of the LCA for Reynolds numbers of 75 and above. As the Reynolds number is increased, the size of the recirculation zone increases and its length approximately doubles for each doubling of the Reynolds number, as does the intensity of the flow.

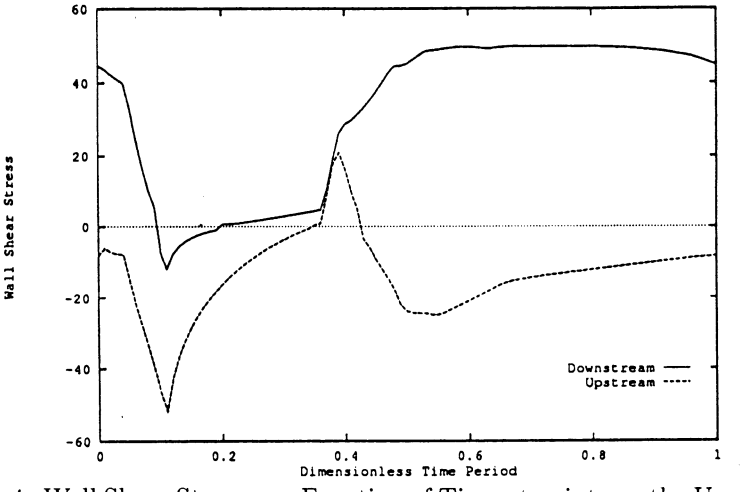


Figure 4: Wall Shear Stress as a Function of Time at points on the Upstream and Downstream Sides of the LCA

The behaviour of the wall shear stress during the transient simulation is best summarised in figure 4. This shows the wall shear stress at points on the upstream and downstream sides of the LCA, two positions of major interest with regard to atheroma formation. The values on the ordinate are really the magnitudes of the wall shear stress with the sign simply indicating whether the local flow is into the LCA (positive) or out of the LCA (negative). As the fluid decelerates, the magnitude of the shear on the downstream side decreases while on the upstream side it increases. During the period of reversed flow the magnitude is much greater on the upstream wall. The shears are of similar magnitude during the rapid acceleration of early diastole. Later in diastole, the downstream wall shear continues to increase, whereas the upstream wall shear firstly dips then changes direction, representing a region of flow separation on the upstream wall. Also from this figure, it is interesting to note that for a great portion of the cardiac cycle, flows on the opposite sides of the LCA are in opposite directions. For more than half of the cardiac cycle there is a region of flow separation on the upstream wall. Further, for the period from approximately $t = 0.20$ until $t = 0.37$ (during the final stages of the reverse flow phase), a region of flow separation exists on the downstream wall. Generally, during diastole, the magnitude of the downstream wall shear stress is greater than that on the upstream side, however, for most of systole, this is reversed.

CONCLUSION

Three dimensional modelling of blood flow through the coronary tree enables wall shear stresses to be computed for a variety of flows and anatomical variants. The results will lead to a knowledge of which flow patterns predispose to fatty streak formation and subsequent atheroma. The present

study and the current hypotheses regarding atheroma formation, narrowing would be expected to form in the entrance to the LCA with other growth on the wall of the left main stem above the entrance to the LCA.

REFERENCES

[1] Fry, D. Acute vascular endothelial changes associated with increased blood velocity gradients. *Circ. Res.*, Vol. 22, pp. 165–197, 1968.

[2] Caro, C. G., Fitz-Gerald, J. M., and Schroter, R. C. Atheroma and arterial wall shear: observation, correlation and proposal of a shear dependent mass transfer mechanism for atherogenesis. *Proc. R. Soc. Lond.*, Vol. B177, pp. 109–159, 1971.

[3] Stary, H. C. Evolution and progression of atherosclerotic lesions in coronary arteries of children and young adults. *Arteriosclerosis*, Vol. 9(1), pp. I–19 - I–32, 1989.

[4] Asakura, T. and Karino, T. Flow patterns and spatial distribution of atherosclerotic lesions in human coronary arteries. *Circ. Res.*, Vol. 66, pp. 1054–1066, 1990.

[5] Rindt, C. C. M., van Steenhoven, A. A., Janssen, J. D., Reneman, R. S., and Segal, A. A numerical analysis of steady flow in a three–dimensional model of the carotid artery bifurcation. *J. Biomechanics*, Vol. 23(5), pp. 461–473, 1990.

[6] Perktold, K. and Resch, M. Numerical flow studies in human carotid artery bifurcations: basic discussion of the geometry factor in atherogenesis. *J. Biomed. Eng.*, Vol. 12, pp. 111–123, March 1990.

[7] Perktold, K., Resch, M., and Peter, R. O. Three–dimensional numerical analysis of the pulsatile flow and wall shear stress in the carotid artery bifurcation. *J. Biomechanics*, Vol. 24(6), pp. 409–420, 1991.

[8] Perktold, K., Nerem, R. M., and Peter, R. O. A numerical calculation of flow in a curved tube model of the left main coronary artery. *J. Biomechanics*, Vol. 24(3–4), pp. 175–189, 1991.

[9] Engelman, M. S. FIDAP - a fluid dynamics analysis package. *Adv. Engng Softw.*, Vol. 4, pp. 163–166, 1982.

[10] Engelman, M. S. *FIDAP User's Guide.* Fluid Dynamics International, Evanston,Illinois, version 5.0 edition, 1990.

[11] Fischer, G. M. and Llaurado, J. G. Collagen and elastin content in canine arteries selected from functionally different vascular beds. *Circ. Res.*, Vol. 19, pp. 394–399, 1966.